Suppression of Hadrons with Large Transverse Momentum in Central Au+Au Collisions at $\sqrt{s_{NN}} = 130$ GeV

K. Adcox,[40] S. S. Adler,[3] N. N. Ajitanand,[27] Y. Akiba,[14] J. Alexander,[27] L. Aphecetche,[34] Y. Arai,[14] S.H. Aronson,[3] R. Averbeck,[28] T. C. Awes,[29] K. N. Barish,[5] P. D. Barnes,[19] J. Barrette,[21] B. Bassalleck,[25] S. Bathe,[22] V. Baublis,[30] A. Bazilevsky,[12,32] S. Belikov,[12,13] F. G. Bellaiche,[29] S. T. Belyaev,[16] M. J. Bennett,[19] Y. Berdnikov,[35] S. Botelho,[33] M. L. Brooks,[19] D. S. Brown,[26] N. Bruner,[25] D. Bucher,[22] H. Buesching,[22] V. Bumazhnov,[12] G. Bunce,[3,32] J. Burward-Hoy,[28] S. Butsyk,[28,30] T. A. Carey,[19] P. Chand,[2] J. Chang,[5] W. C. Chang,[1] L. L. Chavez,[25] S. Chernichenko,[12] C. Y. Chi,[8] J. Chiba,[14] M. Chiu,[8] R. K. Choudhury,[2] T. Christ,[28] T. Chujo,[3,39] M. S. Chung,[15,19] P. Chung,[27] V. Cianciolo,[29] B. A. Cole,[8] D. G. D'Enterria,[34] G. David,[3] H. Delagrange,[34] A. Denisov,[12] A. Deshpande,[32] E. J. Desmond,[3] O. Dietzsch,[33] B. V. Dinesh,[2] A. Drees,[28] A. Durum,[12] D. Dutta,[2] K. Ebisu,[24] Y. V. Efremenko,[29] K. El Chenawi,[40] H. En'yo,[17,31] S. Esumi,[39] L. Ewell,[3] T. Ferdousi,[5] D. E. Fields,[25] S. L. Fokin,[16] Z. Fraenkel,[42] A. Franz,[3] A. D. Frawley,[9] S.-Y. Fung,[5] S. Garpman,[20] T. K. Ghosh,[40] A. Glenn,[36] A. L. Godoi,[33] Y. Goto,[32] S. V. Greene,[40] M. Grosse Perdekamp,[32] S. K. Gupta,[2] W. Guryn,[3] H.-Å. Gustafsson,[20] J. S. Haggerty,[3] H. Hamagaki,[7] A. G. Hansen,[19] H. Hara,[24] E. P. Hartouni,[18] R. Hayano,[38] N. Hayashi,[31] X. He,[10] T. K. Hemmick,[28] J. M. Heuser,[28] M. Hibino,[41] J. C. Hill,[13] D. S. Ho,[43] K. Homma,[11] B. Hong,[15] A. Hoover,[26] T. Ichihara,[31,32] K. Imai,[17,31] M. S. Ippolitov,[16] M. Ishihara,[31,32] B. V. Jacak,[28,32] W. Y. Jang,[15] J. Jia,[28] B. M. Johnson,[3] S. C. Johnson,[18,28] K. S. Joo,[23] S. Kametani,[41] J. H. Kang,[43] M. Kann,[30] S. S. Kapoor,[2] S. Kelly,[8] B. Khachaturov,[42] A. Khanzadeev,[30] J. Kikuchi,[41] D. J. Kim,[43] H. J. Kim,[43] S. Y. Kim,[43] Y. G. Kim,[43] W. W. Kinnison,[19] E. Kistenev,[3] A. Kiyomichi,[39] C. Klein-Boesing,[22] S. Klinksiek,[25] L. Kochenda,[30] V. Kochetkov,[12] D. Koehler,[25] T. Kohama,[11] D. Kotchetkov,[5] A. Kozlov,[42] P. J. Kroon,[3] K. Kurita,[31,32] M. J. Kweon,[15] Y. Kwon,[43] G. S. Kyle,[26] R. Lacey,[27] J. G. Lajoie,[13] J. Lauret,[27] A. Lebedev,[13,16] D. M. Lee,[19] M. J. Leitch,[19] X. H. Li,[5] Z. Li,[6,31] D. J. Lim,[43] M. X. Liu,[19] X. Liu,[6] Z. Liu,[6] C. F. Maguire,[40] J. Mahon,[3] Y. I. Makdisi,[3] V. I. Manko,[16] Y. Mao,[6,31] S. K. Mark,[21] S. Markacs,[8] G. Martinez,[34] M. D. Marx,[28] A. Masaike,[17] F. Matathias,[28] T. Matsumoto,[7,41] P. L. McGaughey,[19] E. Melnikov,[12] M. Merschmeyer,[22] F. Messer,[28] M. Messer,[3] Y. Miake,[39] T. E. Miller,[40] A. Milov,[42] S. Mioduszewski,[3,36] R. E. Mischke,[19] G. C. Mishra,[10] J. T. Mitchell,[3] A. K. Mohanty,[2] D. P. Morrison,[3] J. M. Moss,[19] F. Mühlbacher,[28] M. Muniruzzaman,[5] J. Murata,[31] S. Nagamiya,[14] Y. Nagasaka,[24] J. L. Nagle,[8] Y. Nakada,[17] B. K. Nandi,[5] J. Newby,[36] L. Nikkinen,[21] P. Nilsson,[20] S. Nishimura,[7] A. S. Nyanin,[16] J. Nystrand,[20] E. O'Brien,[3] C. A. Ogilvie,[13] H. Ohnishi,[3,11] I. D. Ojha,[4,40] M. Ono,[39] V. Onuchin,[12] A. Oskarsson,[20] L. Österman,[20] I. Otterlund,[20] K. Oyama,[7,38] L. Paffrath,[3,∗] A. P. T. Palounek,[19] V. S. Pantuev,[28] V. Papavassiliou,[26] S. F. Pate,[26] T. Peitzmann,[22] A. N. Petridis,[13] C. Pinkenburg,[3,27] R. P. Pisani,[3] P. Pitukhin,[12] F. Plasil,[29] M. Pollack,[28,36] K. Pope,[36] M. L. Purschke,[3] I. Ravinovich,[42] K. F. Read,[29,36] K. Reygers,[22] V. Riabov,[30,35] Y. Riabov,[30] M. Rosati,[13] A. A. Rose,[40] S. S. Ryu,[43] N. Saito,[31,32] A. Sakaguchi,[11] T. Sakaguchi,[7,41] H. Sako,[39] T. Sakuma,[31,37] V. Samsonov,[30] T. C. Sangster,[18] R. Santo,[22] H. D. Sato,[17,31] S. Sato,[39] S. Sawada,[14] B. R. Schlei,[19] Y. Schutz,[34] V. Semenov,[12] R. Seto,[5] T. K. Shea,[3] I. Shein,[12] T.-A. Shibata,[31,37] K. Shigaki,[14] T. Shiina,[19] Y. H. Shin,[43] I. G. Sibiriak,[16] D. Silvermyr,[20] K. S. Sim,[15] J. Simon-Gillo,[19] C. P. Singh,[4] V. Singh,[4] M. Sivertz,[3] A. Soldatov,[12] R. A. Soltz,[18] S. Sorensen,[29,36] P. W. Stankus,[29] N. Starinsky,[21] P. Steinberg,[8] E. Stenlund,[20] A. Ster,[44] S. P. Stoll,[3] M. Sugioka,[31,37] T. Sugitate,[11] J. P. Sullivan,[19] Y. Sumi,[11] Z. Sun,[6] M. Suzuki,[39] E. M. Takagui,[33] A. Taketani,[31] M. Tamai,[41] K. H. Tanaka,[14] Y. Tanaka,[24] E. Taniguchi,[31,37] M. J. Tannenbaum,[3] J. Thomas,[28] J. H. Thomas,[18] T. L. Thomas,[25] W. Tian,[6,36] J. Tojo,[17,31] H. Torii,[17,31] R. S. Towell,[19] I. Tserruya,[42] H. Tsuruoka,[39] A. A. Tsvetkov,[16] S. K. Tuli,[4] H. Tydesjö,[20] N. Tyurin,[12] T. Ushiroda,[24] H. W. van Hecke,[19] C. Velissaris,[26] J. Velkovska,[28] M. Velkovsky,[28] A. A. Vinogradov,[16] M. A. Volkov,[16] A. Vorobyov,[30] E. Vznuzdaev,[30] H. Wang,[5] Y. Watanabe,[31,32] S. N. White,[3] C. Witzig,[3] F. K. Wohn,[13] C. L. Woody,[3] W. Xie,[5,42] K. Yagi,[39] S. Yokkaichi,[31] G. R. Young,[29] I. E. Yushmanov,[16] W. A. Zajc,[8] Z. Zhang,[28] and S. Zhou[6]

(PHENIX Collaboration)

[1] Institute of Physics, Academia Sinica, Taipei 11529, Taiwan
[2] Bhabha Atomic Research Centre, Bombay 400 085, India
[3] Brookhaven National Laboratory, Upton, NY 11973-5000, USA
[4] Department of Physics, Banaras Hindu University, Varanasi 221005, India
[5] University of California - Riverside, Riverside, CA 92521, USA
[6] China Institute of Atomic Energy (CIAE), Beijing, People's Republic of China
[7] Center for Nuclear Study, Graduate School of Science, University of Tokyo, 7-3-1 Hongo, Bunkyo, Tokyo 113-0033, Japan
[8] Columbia University, New York, NY 10027 and Nevis Laboratories, Irvington, NY 10533, USA
[9] Florida State University, Tallahassee, FL 32306, USA
[10] Georgia State University, Atlanta, GA 30303, USA
[11] Hiroshima University, Kagamiyama, Higashi-Hiroshima 739-8526, Japan

[12] *Institute for High Energy Physics (IHEP), Protvino, Russia*
[13] *Iowa State University, Ames, IA 50011, USA*
[14] *KEK, High Energy Accelerator Research Organization, Tsukuba-shi, Ibaraki-ken 305-0801, Japan*
[15] *Korea University, Seoul, 136-701, Korea*
[16] *Russian Research Center "Kurchatov Institute", Moscow, Russia*
[17] *Kyoto University, Kyoto 606, Japan*
[18] *Lawrence Livermore National Laboratory, Livermore, CA 94550, USA*
[19] *Los Alamos National Laboratory, Los Alamos, NM 87545, USA*
[20] *Department of Physics, Lund University, Box 118, SE-221 00 Lund, Sweden*
[21] *McGill University, Montreal, Quebec H3A 2T8, Canada*
[22] *Institut für Kernphysik, University of Münster, D-48149 Münster, Germany*
[23] *Myongji University, Yongin, Kyonggido 449-728, Korea*
[24] *Nagasaki Institute of Applied Science, Nagasaki-shi, Nagasaki 851-0193, Japan*
[25] *University of New Mexico, Albuquerque, NM 87131, USA*
[26] *New Mexico State University, Las Cruces, NM 88003, USA*
[27] *Chemistry Department, State University of New York - Stony Brook, Stony Brook, NY 11794, USA*
[28] *Department of Physics and Astronomy, State University of New York - Stony Brook, Stony Brook, NY 11794, USA*
[29] *Oak Ridge National Laboratory, Oak Ridge, TN 37831, USA*
[30] *PNPI, Petersburg Nuclear Physics Institute, Gatchina, Russia*
[31] *RIKEN (The Institute of Physical and Chemical Research), Wako, Saitama 351-0198, JAPAN*
[32] *RIKEN BNL Research Center, Brookhaven National Laboratory, Upton, NY 11973-5000, USA*
[33] *Universidade de São Paulo, Instituto de Física, Caixa Postal 66318, São Paulo CEP05315-970, Brazil*
[34] *SUBATECH (Ecole des Mines de Nantes, IN2P3/CNRS, Universite de Nantes) BP 20722 - 44307, Nantes-cedex 3, France*
[35] *St. Petersburg State Technical University, St. Petersburg, Russia*
[36] *University of Tennessee, Knoxville, TN 37996, USA*
[37] *Department of Physics, Tokyo Institute of Technology, Tokyo, 152-8551, Japan*
[38] *University of Tokyo, Tokyo, Japan*
[39] *Institute of Physics, University of Tsukuba, Tsukuba, Ibaraki 305, Japan*
[40] *Vanderbilt University, Nashville, TN 37235, USA*
[41] *Waseda University, Advanced Research Institute for Science and Engineering, 17 Kikui-cho, Shinjuku-ku, Tokyo 162-0044, Japan*
[42] *Weizmann Institute, Rehovot 76100, Israel*
[43] *Yonsei University, IPAP, Seoul 120-749, Korea*
[44] *KFKI Research Institute for Particle and Nuclear Physics (RMKI), Budapest, Hungary*†
(May 22, 2006)

Transverse momentum spectra for charged hadrons and for neutral pions in the range 1 GeV/c < p_T < 5 GeV/c have been measured by the PHENIX experiment at RHIC in Au+Au collisions at $\sqrt{s_{NN}} = 130$ GeV. At high p_T the spectra from peripheral nuclear collisions are consistent with scaling the spectra from p+p collisions by the average number of binary nucleon-nucleon collisions. The spectra from central collisions are significantly suppressed when compared to the binary-scaled p+p expectation, and also when compared to similarly binary-scaled peripheral collisions, indicating a novel nuclear medium effect in central nuclear collisions at RHIC energies.

PACS numbers: 25.75.Dw

Ultrarelativistic heavy ion collisions provide the opportunity to study strongly interacting matter at high temperature and density. At Brookhaven National Laboratory's Relativistic Heavy Ion Collider (RHIC), nuclei as heavy as gold (Au) are accelerated to energies of $\sqrt{s_{NN}} = 200$ GeV per nucleon-nucleon pair. In the early stages of a central collision, energy densities are expected to be sufficient to dissolve normal nuclear matter into a phase of deconfined quarks and gluons, the "Quark Gluon Plasma" (QGP). The PHENIX experiment is designed to investigate nuclear collisions with a wide variety of probes, focusing primarily on those produced in the early stages of the collision.

Of particular interest are the products of parton scatterings with large momentum transfer ("hard scatterings"). In p+p collisions hard-scattered partons fragment into jets of hadrons; these fragments are the primary source of hadrons at high transverse momentum (p_T), typically above ∼2 GeV/c [1]. In a high-energy nuclear collision hard scattering will occur at the earliest time during the collision, well before the QGP is expected to form, and thus the scattered partons will subsequently experience the strongly interacting medium created in the collision. These partons are expected to lose energy [2] in hot and dense nuclear matter through gluon bremsstrahlung, effectively quenching jet produc-

tion. This would have many observable consequences, of which the most directly measurable would be a depletion in the yield of high p_T hadrons [3]. It has been suggested that the energy loss is larger in a medium of deconfined color charges than in hadronic matter [4], making "jet quenching" a potential signature for QGP formation.

To quantify such modifications we need a baseline expectation for spectra from nuclear (A+A) collisions in the absence of nuclear medium effects. Given that hard parton scatterings have small cross sections, one can regard the nuclei as an incoherent superposition of partons ("point-like scaling"). We approximate this by modelling the A+A collision as a sum of independent nucleon-nucleon (N+N) collisions ("binary scaling"). For a given class of A+A collisions, we can determine $\langle N_{binary} \rangle$ the average number of inelastic N+N collisions per event and then define the *nuclear modification factor* as the ratio,

$$R_{AA}(p_T) = \frac{(1/N_{evt}) \, d^2 N^{A+A}/dp_T d\eta}{(\langle N_{binary} \rangle / \sigma_{inel}^{N+N}) \, d^2 \sigma^{N+N}/dp_T d\eta}. \quad (0.1)$$

In the absence of nuclear modifications to hard scattering, the ratio R_{AA} will be unity; thus departures from $R_{AA} = 1$ indicate nuclear medium effects. Previous measurements indicate that for p_T below 2 GeV/c, R_{AA} is smaller than one since the bulk of particle production scales with the number of nucleons participating in the reaction [5,6]. For p_T above 2 GeV/c particle production in p+A collisions is enhanced compared to binary scaling, commonly referred to as the "Cronin effect" [7]. Parton shadowing as measured in lepton+A collisions [8] is also expected to modify the hadron spectra in p+A and A+A compared to binary scaling.

We examine high-p_T spectra of charged hadrons and neutral pions measured by the PHENIX experiment [9,10] in a central and a peripheral class of Au+Au collisions at $\sqrt{s_{NN}} = 130$ GeV. These data are obtained with the central spectrometer, which consists of two arms, "east" and "west", each covering $\Delta\phi = 90^o$ and $|\eta| < 0.35$. The arms are positioned outside an axially-symmetric magnetic field centered around the beam axis.

Charged particles are reconstructed using a drift chamber (DC) and two layers of multi-wire proportional chambers with pad-readout (PC1, PC3) in the east arm. The DC measures the particle trajectories between 2.0 and 2.4 m radius in the plane perpendicular to the beam axis. A matching hit in PC1 at ∼ 2.5 m, together with location of the collision vertex, fixes the polar angle. Particle momenta are determined with a resolution of $\delta p/p \simeq 0.6\% \oplus 3.6\% \, p$ (GeV/c). The absolute momentum scale is known to better than 2%. Trajectories are confirmed by requiring a matching hit within a $\pm 2\sigma$ window (about 2.5 cm) in PC3 at a radius of 5 m, which eliminates nearly all secondary tracks from decays and interactions in material. The remaining background is due primarily to accidental associations. The level of

background to signal is negligible below $p_T < 2$ GeV/c, rises to 1/10 at 3.5 GeV/c, and reaches 1/1 at 6 GeV/c. This background is measured statistically, by swapping the z-coordinate of the PC3 hits, and subtracted from the yield.

Corrections for acceptance, reconstruction efficiency, decays in flight, momentum resolution, and dead areas are determined using a full GEANT simulation. Simulated single particles are embedded in real events to model the effect of detector occupancy. In peripheral Au+Au collisions the track reconstruction efficiency exceeds 98%, while it is reduced to $68 \pm 6\%$ for central collisions, independent of momentum. Corrections due to finite momentum resolution are negligible at low p_T and rise to the level of 30% at 5 GeV/c. The systematic errors (Table I) are dominated by the uncertainty in the Monte Carlo description of the detector, including the dead areas and the momentum resolution.

Neutral pions are measured via their $\pi^0 \rightarrow \gamma\gamma$ decay. Two separate analyses are performed, the first using a lead-scintillator (PbSc) sampling calorimeter in half ($\Delta\phi = 45^o$) of the west arm aperture and the second with a lead-glass Cerenkov (PbGl) calorimeter in a quarter ($\Delta\phi = 22.5^o$) of the east arm aperture. The two analyses have very different systematics, and Figure 1 shows the agreement of their final π^0 spectra.

In both analyses, pairs of calorimeter showers are binned in pair p_T and invariant mass $m_{\gamma\gamma}$. The energy scale is verified using both the π^0 mass and E/p ratio for identified electrons and is known to < 1.5% [11]. Hadron-induced showers are suppressed with arrival time and shower shape cuts. The combinatorial pair background is estimated by mixing showers from different events with similar centrality. The mixed $m_{\gamma\gamma}$ distribution is subtracted from the true distribution after being normalized in a region outside the π^0 mass peak. The π^0 yield in each p_T bin is determined by integrating the subtracted $m_{\gamma\gamma}$ distribution in a window determined by a Gaussian fit to the π^0 peak.

The π^0 spectra are corrected for losses due to energy resolution, cluster overlaps, analysis cuts, dead detector areas, and acceptance. Smearing of the photon energy due to resolution and cluster overlaps is used to simulate the $m_{\gamma\gamma}$ peak at each p_T, which agrees with that seen in the data. To estimate the π^0 reconstruction efficiency, the same cuts are applied to the simulated $m_{\gamma\gamma}$ distributions as applied to the real data.

Contributions to the yield from pions not originating from the vertex are estimated by GEANT simulation to be 6-8%. The dominant sources of error are the uncertainty in the particle identification, the effect of energy smearing, and the peak extraction procedure. Their relative contributions to the total errors (see Table I) differ for the two analyses.

Event classification is provided by the combination of two beam-beam counters (BBC's) and two zero-degree

calorimeters (ZDC's). We present data from two event samples, central and peripheral. The central sample covers the 0–10% most central fraction of the geometrical Au+Au cross-section, while the peripheral sample contains events in the 60–80% selection. Using a Glauber model combined with a simulation of the BBC and ZDC responses [5], we estimate $\langle N_{binary} \rangle = 905 \pm 96$ for the central sample, $\langle N_{binary} \rangle = 20 \pm 6$ for the peripheral sample, and 45 ± 13 for the ratio between them. The errors include the uncertainties in the parameters used in the Glauber model [12], as well as in the fraction of the total geometrical cross section ($92 \pm 4\%$) seen by the interaction trigger [13].

The p_T distributions for charged hadrons and neutral pions are shown for both centrality classes in Fig. 1. In this figure, those following, and Table I, the systematic errors shown are the quadrature sums of conservatively estimated limits on several independent errors and represent upper bounds on standard deviations. They are also substantially correlated between points.

The data are compared to the binary-scaled yield from N+N collisions. Since no N+N data exist at $\sqrt{s}$ =130 GeV, we parameterize the cross section $1/(2\pi p_T) d^2\sigma/d\eta dp_T$ for $(h^+ + h^-)/2$ as $A/(1 + p_T/p_0)^n$. We determine the parameters A=330 mb/GeV^2/c^2, p_0=1.72 GeV/c, and n=12.4 by interpolating between results from p+p collisions at the ISR [14] and $\overline{p}$+p collisions at the Sp$\overline{p}$S [15] and the Tevatron [16]. The systematic error in the N+N reference (Table I) is due to the error in the absolute normalization of the data used and in the interpolation technique. For neutral pions we scale the charged hadron cross section by the charged pion to charged hadron ratio π/h observed at the ISR [14]. This was found to be 0.63 ± 0.06 nearly independent of p_T above 1.5 GeV/c.

For $p_T > 2$ GeV/c the binary-scaling prediction agrees with the data from peripheral collisions for both charged and neutrals, while for central collisions the data lie noticeably below the prediction. To examine this difference more directly, we plot the ratio R_{AA} for central collisions in Fig. 2. For the charged spectrum R_{AA} rises up to 2 GeV/c, as expected; but above 2 GeV/c R_{AA} remains significantly below unity for both spectra.

The depletion is quite striking, since the production of high-p_T hadrons in p+A collisions at fixed-target energies is known to be enhanced compared to the binary-scaling expectation for $p_T > 2$ GeV/c, i.e., the Cronin effect [7]. A similar enhancement has also been observed in heavy ion collisions at lower energies [17,18], as shown in Fig. 2. Phenomenological calculations [17] including shadowing and the Cronin effect predicted that for central Au+Au collisions at $\sqrt{s_{NN}}$=130 GeV, $R_{AA} > 1$ for hadron spectra in the p_T range 3–9 GeV/c with a peak value of $R_{AA} \simeq 1.3$ at 4 GeV/c.

Above 2 GeV/c R_{AA} is lower for pions than for charged hadrons, which implies that the π/h ratio is smaller in central RHIC Au+Au collisions than in ISR p+p collisions. This is consistent with identified charged hadron spectra measured by PHENIX [19] for which a large yield of protons and antiprotons is observed at $p_T \sim 2$ GeV/c.

We can also examine the spectra from central collisions for modifications at high p_T by comparing them to the spectra from peripheral collisions after dividing each by the corresponding values of $\langle N_{binary} \rangle$. The central-to-peripheral ratio is a useful complement to R_{AA}, since it should be unity in the limit of point-like scaling. Many of the experimental uncertainties are reduced in this ratio (see Table I). Additionally, the uncertainty induced by the p+p interpolation is eliminated, albeit at the expense of incurring that in $\langle N_{binary} \rangle$ for the peripheral class. We note that there may be effects from the centrality dependence of nuclear shadowing and/or the Cronin effect that would also be present in this comparison.

The central-to-peripheral ratios are plotted in Fig. 3. Like R_{AA} this ratio is below unity at all observed p_T for both charged hadrons and neutral pions, indicating a suppression of the yield per N+N collision in central collisions relative to peripheral. The difference between the two ratios implies that the π/h ratio is smaller in central collisions than in peripheral.

We have presented spectra for charged hadrons and neutral pions measured at 90° from central and peripheral Au+Au collisions in the PHENIX experiment at RHIC. Above $p_T \sim 2$ GeV/c, the spectra from peripheral collisions appear to be consistent (albeit within a substantial systematic error) with a simple, incoherent sum of underlying N+N collisions. The spectra from central collisions, in contrast, are systematically below the scaled N+N expectation, both when compared to data from p+p collisions and to spectra from Au+Au peripheral collisions. The suppression in central collisions is in qualitative agreement with the predictions of energy loss by scattered partons traversing a dense medium. However, other nuclear medium effects should be understood before a quantitative conclusion can be drawn. Measurements in p+A at RHIC can help in this direction.

*   Deceased
†   Not a participating institution.

[1] J.F. Owens et al., Phys. Rev. **D18**, 1501 (1978).

[2] M. Gyulassy and M. Plümer, Phys. Lett. **B243**, 432 (1990); R. Baier et al., Phys. Lett. **B345**, 277 (1995).

[3] X.N. Wang and M. Gyulassy, Phys. Rev. Lett. **68**, 1480 (1992); X.N. Wang, Phys. Rev. **C58**, 2321 (1998).

[4] R. Baier, D. Schiff and B.G. Zakharov, Annu. Rev. Nucl. Part. Sci. **50**, 37 (2000).

[5] K. Adcox et al., Phys. Rev. Lett. **86**, 3500 (2001).

[6] C. Adler et al., Phys. Rev. Lett. **87**, 112303 (2001).

[7] D. Antreasyan et al., Phys. Rev. **D19**, 764 (1979).

[8] J.J. Aubert et al., Phys. Lett. **B123**, 275 (1983); R.G. Arnold et al., Phys. Rev. Lett. **52**, 727 (1984).

[9] PHENIX Collaboration, D. Morrison, et al., Nucl. Phys. **A638**, 565c (1998).

[10] PHENIX Collaboration, W. Zajc, et al., Quark Matter 2001, Nucl. Phys. **A** (to be published).

[11] K. Adcox et al., Phys. Rev. Lett. **87**, 052301 (2001).

[12] We use the Woods-Saxon parameters radius = $6.38^{+0.27}_{-0.13}$ fm, diffusivity = 0.53 ± 0.01 fm [B. Hahn, D.G. Ravenhall and R. Hofstadter, Phys. Rev. **101**, 1131 (1956)], and $\sigma^{inel}_{N+N} = 40 \pm 3$ mb.

[13] The error due to model uncertainties is 2% [5]. An additional 3.5% error results from time dependencies in the centrality selection over the large data sample.

[14] B. Alper et al., Nucl. Phys. **B100**, 237 (1975).

[15] C. Albajar et al., Nucl. Phys. **B335**, 261 (1990).

[16] F. Abe et al., Phys. Rev. Lett. **61**, 1819 (1988).

[17] E. Wang & X.N. Wang, Phys. Rev. **C64**, 034901 (2001) and references therein.

[18] A.L.S. Angelis et al., Phys. Lett. **B185**, 213 (1987).

[19] PHENIX Collaboration, J. Velkovska et al., Quark Matter 2001, Nucl. Phys. **A** (to be published).
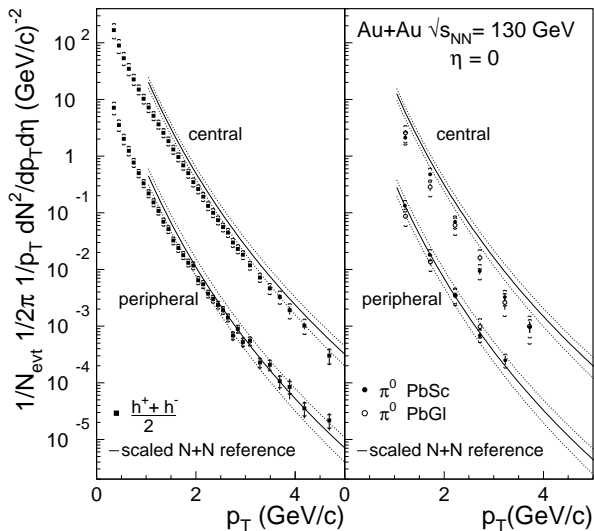
FIG. 1. The yields per event at mid-rapidity for charged hadrons (*left*) and neutral pions (*right*) are shown as a function of p_T for 60–80% (*lower*) and 0–10% (*upper*) event samples. The error bars indicate the statistical errors on the yield; the surrounding brackets indicate the systematic errors. Also shown are the N+N references for charged hadrons and neutral pions, each scaled up by $\langle N_{binary} \rangle$ for the class. The bands indicate the uncertainty in the N+N reference and in the $\langle N_{binary} \rangle$.
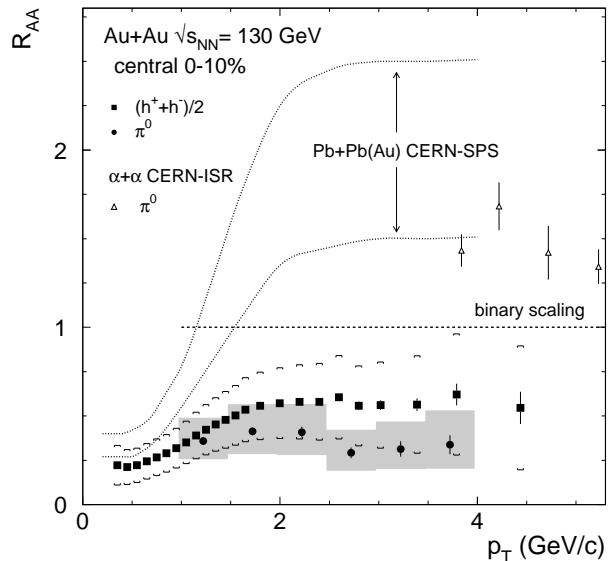

FIG. 2. The ratio R_{AA} for charged hadrons and neutral pions (weighted average of PbSc and PbGl results) in central Au+Au collisions. The error bars indicate the statistical errors on the measurement. The surrounding bands [shaded for π^0's, brackets for $(h^+ + h^-)/2$] are the quadrature sums of (i) the systematic errors on the measurement, (ii) the uncertainty in the N+N reference, and (iii) the uncertainty in $\langle N_{binary} \rangle$. Also shown are the ratio of inclusive cross sections in $\alpha + \alpha$ compared to p+p at $\sqrt{s_{NN}} = 31$ GeV [18], and spectra from central Pb+Pb, Pb+Au compared to p+p collisions at $\sqrt{s_{NN}} = 17$ GeV [17] shown as a band indicating the range of uncertainty.
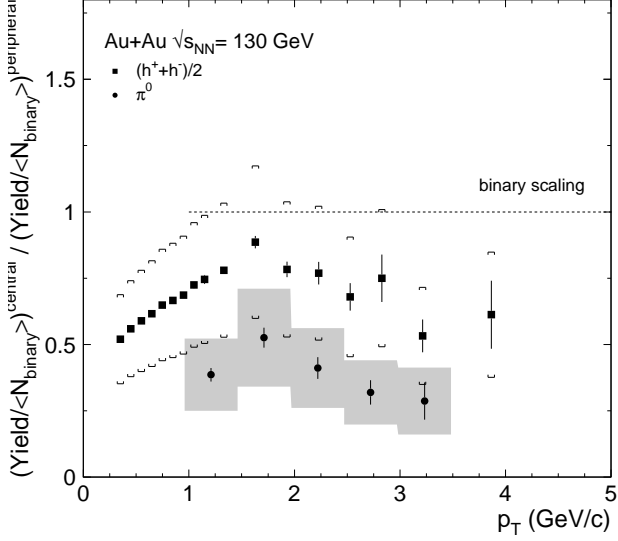
FIG. 3. Ratio of yield per event in central *vs* peripheral Au+Au collisions, with each divided by $\langle N_{binary} \rangle$ for that class. For π^0 the weighted average of PbSc and PbGl results is shown. The error bars indicate the statistical errors on the spectra. The surrounding bands [shaded for π^0's, brackets for $(h^+ + h^-)/2$] are the quadrature sums of (i) the parts of the systematic errors on the spectra that do not cancel in the ratio, and (ii) the uncertainty in $\langle N_{binary} \rangle$ (see Table I).

TABLE I. Relative systematic errors on hadron yields and central-to-peripheral ratios. The errors are quoted for representative p_T and vary between the values shown. For the charged hadron (h) data the errors are highly correlated in p_T for both yields and ratios. For the π^0 data, approximately half of the error in the yield is perfectly correlated in p_T, and some correlation remains in the ratio.

Sys. error:	Yield	p_T [GeV/c]	Cent/Per	p_T [GeV/c]
h data	27%	0.5	8%	all
	16-18%	0.8-3.5		
	30%	4.7		
π^0 data	25%	1.2	24%	1.2
(PbSc)	35%	3.7	33%	3.2
π^0 data	33%	1.2	32%	1.2
(PbGl)	52%	3.7	40%	2.7
π^0 data	21%	1.2	20%	1.2
(combined)	30%	3.7	24%	2.7
N+N ref.	20%	1.0	N/A	
	35%	5.0		
$\langle N_{binary} \rangle$			29%	all
central	11%	all		
peripheral	30%	all		